Journal of
Applied Crystallography

ISSN 0021-8898

Received 9 May 2006
Accepted 28 November 2006

Improvement of data treatment in small-angle neutron scattering

Annie Brûlet,* Didier Lairez, Alain Lapp and Jean-Pierre Cotton

Laboratoire Léon Brillouin, CEA-Saclay, 91191 Gif-sur-Yvette Cedex, France. Correspondence e-mail: brulet@llb.saclay.cea.fr

Small-angle neutron scattering has been successfully used since the 1970s. As a general rule, methods to extract the useful signal from that received by the detector are well known and give good results. At the Laboratoire Léon Brillouin, for example, these methods have been employed for a long time. However, the data reduction software has been changed for the following reasons. Problems are encountered if the container of the sample gives a spurious signal or if the scattering angle is so large that its cosine cannot be approximated by 1. In the present paper, generalizations of formulas are made in order to account for these difficulties. The decrease of scattered intensity delivered by an incoherent sample that is often observed at large angles is shown to be only due to a geometrical effect. The consequent modifications of the relations used for the normalization of cells of position-sensitive detectors and for the absolute calibration are given. As for the inherent background of the sample, the contribution of density fluctuations is usually neglected. This contribution is formally given as a function of the contrast lengths and of the isothermal compressibility of the sample. This new result allows numerical evaluations of the different terms of the inherent sample background. Practical examples are given. Finally, several methods, developed at the Laboratoire Léon Brillouin, are given to determine the background properly. They are based on systematic measurements of transmissions and background levels of suitably prepared blank samples.

© 2007 International Union of Crystallography
Printed in Singapore – all rights reserved

1. Introduction

Small-angle neutron scattering (SANS) is an efficient tool to study nanostructures at typical length scales ranging from 1 to 100 nm. This technique was developed through pioneering work of the 1970s (Cotton *et al.*, 1972; Stuhrmann, 1974; Schmatz *et al.*, 1974; Jacrot, 1976; Kostorz, 1979). It is nowadays widely used to determine characteristic sizes, molecular weights, interactions, shapes and internal structures of macromolecules, aggregates, colloids, biological systems and inorganic materials.

The basics of SANS are now well known and taught in textbooks (Kostorz, 1979; Feigin & Svergun, 1987; Higgins & Benoît, 1994). The primary steps of raw data reduction are widely inspired by those of small-angle X-ray scattering (Guinier, 1964; Cotton *et al.*, 1974) and absolute calibration methods are commonly used to determine the differential scattering cross section in absolute units (Wignall & Bates, 1987; Cotton, 1991*b*; Lindner, 2002). However, prior to any data analysis and comparison with physical models, it is necessary to extract from the measured count rate the quantity that is related to the space correlations of heterogeneities (*e.g.* concentration fluctuations).

Actually, the first step of data treatment amounts to background subtraction. There are two categories of background: external (environmental background, electronic noise, direct beam overflowing, *i.e.* beam tail, scattering from sample container) and inherent to the sample (incoherent scattering, sample compressibility). The usual procedure consists of subtracting the intensity scattered by a blank sample from that of the sample under study (Rawiso *et al.*, 1987; Wignall & Bates, 1987; Cotton, 1991*b*; Calmettes, 1999; Lindner, 2002). This generally gives good results. The approximations used are (i) the scattering angle θ is so small that $\cos\theta = 1$, (ii) the sample container gives no signal and (iii) the sample is incompressible. These approximations are sometimes not reasonable. This paper aims to state their relevance and give improved formulas for continuous neutron sources in the context of the single scattering approximation.

In the following, we describe the different steps to extract from the measured raw data the differential scattering cross section of heterogeneities of a sample, *i.e.* its coherent scattering cross section. First, we explain how to access the total scattering cross section of the sample. The case of a sample in a container is fully treated, as well as corrections for large scattering angles ($\theta > 10^\circ$). It then remains to extract the

signal related to the space correlation of heterogeneities. We show that isothermal compressibility in a multi-component system is not always negligible. Subtraction of the inherent background of the sample is also often complicated by multiple scattering effects that are difficult to calculate in a general way. These problems are widely encountered in most samples of soft matter. In this field especially, it is possible to overcome these difficulties by using appropriate blank samples; their choice and the determination of the background signal are discussed in §3. Finally, for some specific cases, we describe practical methods to determine systematically the inherent background of the sample.

2. From raw data to coherent differential scattering cross section

2.1. Recall: usual data reduction for sample without container

Let us denote $\sigma_s(q)$ as the total scattering cross section of a sample of volume V, with Ω as the solid angle. The differential scattering cross section per volume unit $\tilde{\sigma}_s(q)$ is

$$\tilde{\sigma}_s(q) = \frac{1}{V}\frac{d\sigma_s}{d\Omega}. \quad (1)$$

The magnitude of the scattering vector $\mathbf{q}$ is defined by

$$q = (4\pi/\lambda)\sin(\theta/2), \quad (2)$$

where θ is the scattering angle and λ the neutron wavelength. Classically, assuming scattering at a small angle θ, the approximation $\cos\theta \simeq 1$ allows us to write the intensity $I_s(\theta)$ scattered by a sample of thickness z_s as (Guinier, 1964)

$$I_s(\theta) = \Phi(\lambda)A\epsilon(\lambda)\Delta\Omega \int_0^{z_s} dx\, \exp(-\mu_s x)\,\tilde{\sigma}_s(q)\,\exp[-\mu_s(z_s - x)], \quad (3)$$

where Φ is the neutron beam flux (number per time and surface units), A the sample area exposed to the neutron beam, $\epsilon(\lambda)$ the detector efficiency, $\Delta\Omega$ the detector cell solid angle, x the position of the sample layer where scattering occurs (see Fig. 1), and μ_s the linear attenuation coefficient of the sample for neutrons. The term $\exp[-\mu_s(z_s - x)]$ accounts for the attenuation of scattered neutrons due to absorption and multiple scattering. Equation (3), commonly used, is valid as long as multiple scattering is spread over a wide solid angle and thus remains negligible at small angles.

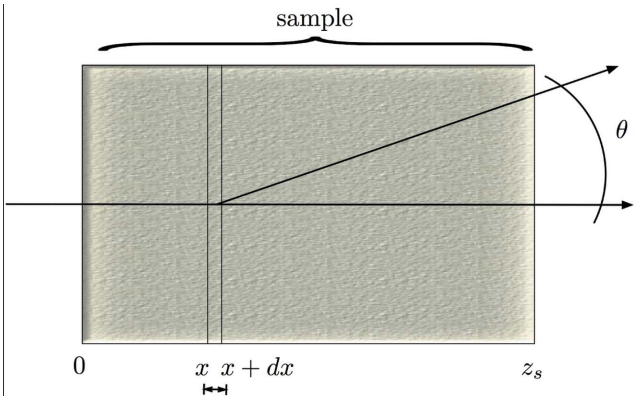

Figure 1
Scattering at angle θ, by a layer of thickness dx situated at distance x from the incoming face of a sample of thickness z_s.

Equation (3) yields the classical expression

$$\begin{aligned} I_s(\theta) &= \Phi(\lambda)A\epsilon(\lambda)\Delta\Omega\, z_s \exp(-\mu_s z_s)\,\tilde{\sigma}_s(\theta) \\ &= z_s T_s C(\lambda)\tilde{\sigma}_s(\theta) \\ &= z_s T_s F_s(\theta). \end{aligned} \quad (4)$$

The subscript s denotes the sample. In practice, $I_s(\theta)$ is the measured count rate, the transmission $T_s = \exp(-\mu_s z_s)$ is measured during the experiment and the sample thickness z_s is known. Determination of the calibration constant $C(\lambda) = \Phi(\lambda)A\epsilon(\lambda)\Delta\Omega$ is required to obtain $\tilde{\sigma}_s(\theta)$ in absolute units (cm^{-1}).

In the absence of the sample, the collimated beam reaches the detector. Most of the beam is normally absorbed by a beamstop, except the beam tail, which gives the corresponding intensity, $F_b(\theta)$. In addition, an external background signal B (electronic noise plus cosmic and ambiance neutrons coming from neutron guides and other spectrometers) is recorded. Then, the count rate recorded without a sample is

$$I_b(\theta) = F_b(\theta) + B.$$

Through the sample, this contribution is reduced to $T_s F_b(\theta) + B$. Thus, the scattered intensity of a sample is

$$I_s(\theta) = z_s T_s F_s(\theta) + T_s F_b(\theta) + B. \quad (5)$$

In SANS, the scattering function $F_s(\theta)$ is the sum of a coherent signal and an incoherent term independent of q. The coherent term (see §3) has two contributions: (i) space correlations of heterogeneities, which is the information that the experimentalist is looking for in most cases; (ii) density fluctuations that display correlation lengths smaller than q^{-1} in SANS and thus give a q-independent contribution. The sum of the two q-independent contributions (incoherent plus density fluctuations) is the inherent background of the sample. In order to estimate this background, the scattered intensity, I_{bk}, of a blank sample is usually measured. Using subscript bk to denote the blank sample, we obtain, following equation (5),

$$I_{bk}(\theta) = z_{bk} T_{bk} F_{bk}(\theta) + T_{bk} F_b(\theta) + B. \quad (6)$$

The choice of an appropriate blank sample is difficult. It is discussed in §3.

Finally, combination of equations (5) and (6) gives the major formula of SANS data treatment:

$$F_s(\theta) - F_{bk}(\theta) = \frac{I_s(\theta) - B}{z_s T_s} - \frac{I_{bk}(\theta) - B}{z_{bk} T_{bk}} - \left(\frac{1}{z_s} - \frac{1}{z_{bk}}\right) F_b(\theta). \quad (7)$$

In practice, measurements of $I_s(\theta)$, $I_{bk}(\theta)$, $I_b(\theta)$ and B are necessary to determine the scattering function $F_s(\theta)$. External background B is measured by placing a strong absorbent (cadmium or B_4C) at the sample position. Equation (7) clearly shows that measurement of $F_b(\theta)$ without a sample is neces-

sary as soon as the sample and its blank have a different thickness. This is often the case with solid samples.

Generally, equation (7) is also used for a sample inside a container, since the container contribution to scattered intensity is expected to be accounted for by the blank sample subtraction. As discussed below, in some cases this is not correct.

2.2. Correction of the approximation $\cos\theta = 1$

As mentioned above, equations (3) and (4) are valid for small angles, when $\cos\theta$ is close to unity. For large angles, corrections must be applied. Actually, for a typical detector at a distance $D \simeq 2$ m from the sample, the maximum scattering angle can be greater than 10° ($\cos\theta \simeq 0.95$). Thus, for experiments performed at smaller distances, the approximation $\cos\theta \simeq 1$ is not recommended, especially if important information is determined from high q range data, where the signal-to-noise ratio is generally weak.

Three parameters in equation (4) depend on $\cos\theta$: detector cell solid angle, detector efficiency (Lindner *et al.*, 2000) and attenuation of the neutron beam scattered at the angle θ. The first two parameters play a role in the calibration constant $C(\lambda)$; the correction to apply is discussed in §2.4.2. The present section is concerned with the angle dependence of the beam attenuation (Calmettes, 1999).

Let us consider neutrons scattered with probability $\tilde{\sigma}(\theta, \lambda)$, at an angle θ, by a sample layer at abscissa x (see Fig. 1). The beam intensity at this abscissa is attenuated by upstream layers, whereas downstream layers contribute to attenuation of the scattered intensity [see equation (3)]. This latter attenuation depends on the actual sample thickness, $(z_s - x)/\cos\theta$, in this direction (Guinier, 1964). Thus equation (3) can be replaced by

$$I_s(\theta) = \Phi(\lambda) A \epsilon(\lambda) \Delta\Omega \int_0^{z_s} \mathrm{d}x \exp(-\mu_s x)\, \tilde{\sigma}_s(q) \exp\left(-\mu_s \frac{z_s - x}{\cos\theta}\right). \tag{8}$$

This equation amounts to writing the beam attenuation as $\int_0^z \mathrm{d}x \exp(-\mu_s x) \exp[-\mu_s(z_s - x)/\cos\theta]$. Assuming $\cos\theta = 1$, this latter integral equals $z\exp(-\mu z) = zT$ and is independent of θ. When this assumption is not valid, this integral becomes $zT(\theta)$ with

$$T(\theta) = T\frac{1 - T^{a(\theta)}}{-a(\theta)\ln(T)} \quad \text{and} \quad a(\theta) = \frac{1}{\cos\theta} - 1. \tag{9}$$

Here, $\ln(T)$ has been introduced in order to express $T(\theta)$ as a function of transmission T measured at $\theta = 0$ (Calmettes, 1999). From a computational point of view, note that for $\theta \to 0$ and/or $T \to 1$, $T(\theta) \to T$ is a ratio of two quantities that tend to 0. In order to be easily calculated, equation (9) can be replaced by the expansion

$$T(\theta) = T\mathcal{E}_1[a(\theta)\ln(T)], \tag{10}$$

with $\mathcal{E}_1(x) = 1 + x/2 + x^2/6 + x^3/24 + x^4/120 + \ldots$, which is calculated in practice up to the fourth order.

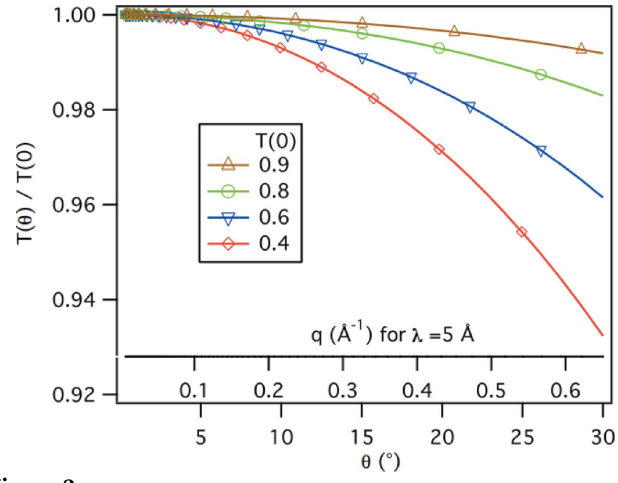

Figure 2
Scattering angle dependence, $T(\theta)/T(0)$, of the sample transmission calculated following equation (9) for different values of the zero-angle measured transmission $T(0)$. The upper abscissa axis corresponds to the scattering vector q for $\lambda = 5$ Å.

The scattering angle dependence of the transmission is more important for low $T(0)$ and high θ. Fig. 2 shows some examples. The angle of dependence of transmission is negligible for $T(0) \gtrsim 0.8$, but has to be considered for lower $T(0)$, especially at high q. Moreover, the angle dependence of the transmission also influences the contribution, $F_b(\theta)$, of the beam tail to the measured scattered intensity. Equation (7) can be generalized

$$F_s(\theta) - F_{bk}(\theta) = \frac{I_s(\theta) - B}{z_s T_s(\theta)} - \frac{I_{bk}(\theta) - B}{z_{bk} T_{bk}(\theta)} - \left[\frac{T_s^{a(\theta)}}{z_s} - \frac{T_{bk}^{a(\theta)}}{z_{bk}}\right] F_b(\theta). \tag{11}$$

This correction for attenuation at high scattering angles ($\theta > 10^\circ$) and its effect on subtraction of the beam without a sample are often missing in SANS data reduction procedures.

2.3. Scattering by a sample inside a container

In the case of a sample inside a container, we have to subtract from the measured scattered intensity the contribution, $I_{EC}(\theta)$, of the empty container. The calculation is given in Appendix *A* for a container with two windows (before and after the sample with respect to the neutron beam) made in the same material and having the same thickness. It is assumed that (i) there is no correlation between the atoms of the sample and those of the container and (ii) multiple scattering has a negligible contribution to the scattered intensity but may only attenuate scattered intensity [see equations (3) and (8)].

Uppercase subscript S denotes the sample in its container, whereas lowercase subscript s denotes the same sample without container. In Appendix *A*, we demonstrate that the scattered intensity is

$$F_s(\theta) = \frac{I_S(\theta) - B}{z_s T_S \alpha_S(\theta)} - \gamma_S(\theta)\left[\frac{I_{EC}(\theta) - B}{\beta_{EC}(\theta) T_{EC}}\right] + \gamma_S(\theta)\left[\frac{T_{EC}^{a(\theta)}}{\beta_{EC}(\theta)} - \frac{T_S^{a(\theta)}}{\beta_S(\theta)}\right] F_b(\theta). \quad (12)$$

The dimensionless quantities $\alpha_S(\theta)$ and $\beta_S(\theta)$ tend to 1 for $\theta \to 0$ and/or $T \to 1$. They are defined by

$$\alpha_S(\theta) = T_{EC}^{a(\theta)/2} \frac{-\left(T_S/T_{EC}\right)^{a(\theta)}}{-a(\theta)\ln\left(T_S/T_{EC}\right)} = \mathcal{E}_2\left[a(\theta)\ln\left(T_{EC}\right)\right] \times \mathcal{E}_1\left[a(\theta)\ln\left(T_S/T_{EC}\right)\right] \quad (13)$$

and

$$\beta_S(\theta) = \left[1 + \left(\frac{T_S}{T_{EC}^{1/2}}\right)^{a(\theta)}\right] \times \frac{1 - T_{EC}^{a(\theta)/2}}{-a(\theta)\ln(T_{EC})} = \mathcal{E}_3\left[a(\theta)\ln\left(T_S/T_{EC}^{1/2}\right)\right] \mathcal{E}_4[a(\theta)\ln(T_{EC})], \quad (14)$$

with $\mathcal{E}_2(x) = 1 + x/2 + x^2/8 + x^3/48 + x^4/384 + \ldots$, $\mathcal{E}_3(x) = 1 + x/2 + x^2/4 + x^3/12 + x^4/48 + \ldots$ and $\mathcal{E}_4(x) = 1 + x/4 + x^2/24 + x^3/192 + x^4/1920 + \ldots$. The quantity $\gamma_S(\theta)$ has the dimension of a reverse thickness. It is defined as

$$\gamma_S(\theta) = \frac{1}{z_s}\frac{\beta_S(\theta)}{\alpha_S(\theta)}. \quad (15)$$

From the above expansions of $\alpha_S(\theta)$ and $\beta_S(\theta)$, one can see that $\gamma_S(\theta)$ benefits from cancellation of opposite variations with θ. In practice

$$\gamma_S(\theta) \simeq 1/z_s. \quad (16)$$

Equations (12)–(15) only use measurable quantities such as transmission of the container, T_{EC}, and transmission of the sample inside its container, T_S, which is related to the actual transmission T_s by $T_S = T_{EC}T_s$. The same formulas also apply to the blank sample $F_{bk}(\theta)$. Finally, the difference $F_s(\theta) - F_{bk}(\theta)$ is

$$F_s(\theta) - F_{bk}(\theta) = \frac{I_S(\theta) - B}{z_s T_S \alpha_S(\theta)} - \frac{I_{BK}(\theta) - B}{z_{bk} T_{BK} \alpha_{BK}(\theta)} - \frac{I_{EC}(\theta) - B}{\beta_{EC}(\theta) T_{EC}}\left[\gamma_S(\theta) - \gamma_{BK}(\theta)\right] + F_b(\theta)\left\{\frac{T_{EC}^{a(\theta)}}{\beta_{EC}(\theta)}\left[\gamma_S(\theta) - \gamma_{BK}(\theta)\right] + \frac{T_{BK}^{a(\theta)}}{z_{bk}\alpha_{BK}(\theta)} - \frac{T_S^{a(\theta)}}{z_s \alpha_S(\theta)}\right\}. \quad (17)$$

The subscript BK denotes the blank sample inside the container. We can see from this equation that, in most cases, measurements of the empty container as well as of the beam without sample are both required. Equation (17) should be used systematically in all treatments of SANS data. The program *PAsidur-PRO* (Lairez, 2006) at the Laboratoire Léon Brillouin (LLB) now performs all these corrections.

In the case of sample and blank of the same thickness, equation (16) allows us to simplify equation (17) to

$$F_s(\theta) - F_{bk}(\theta) = \frac{I_S(\theta) - B}{z_s T_S \alpha_S(\theta)} - \frac{I_{BK}(\theta) - B}{z_{bk} T_{BK} \alpha_{BK}(\theta)} - F_b(\theta)\left[\frac{T_S^{a(\theta)}}{z_s \alpha_S(\theta)} - \frac{T_{BK}^{a(\theta)}}{z_{bk}\alpha_{BK}(\theta)}\right]. \quad (18)$$

Measurement of the beam without sample is still necessary.

At small angles, *i.e.* for $\cos\theta \simeq 1$, equation (17) simplifies to

$$F_s(\theta) - F_{bk}(\theta) = \frac{I_S(\theta) - B}{z_s T_S} - \frac{I_{BK}(\theta) - B}{z_{bk} T_{BK}} - \left(\frac{1}{z_s} - \frac{1}{z_{bk}}\right)\frac{I_{EC}(\theta) - B}{T_{EC}}. \quad (19)$$

In this case, and if the sample and blank thicknesses differ, only measurement of the scattering of the empty container is needed.

In order to test the efficiency of equation (17) for data reduction, the scattered intensity of a solid sample made of a mixture of 2% (*v*/*v*) deuterated polystyrene (PSD) and 98% (*v*/*v*) non-deuterated polystyrene (PSH) inside an aluminium alloy container of 2×1.5 mm thickness was measured. Because of the grain boundaries of metallic alloys, the container significantly contributes to the measured signal at small angles (see Fig. 3). Nevertheless, such materials are frequently used in shear cells, in pressure devices, in supra-conducting magnets or for other sample environments. Measurements were performed at $\lambda = 6$ Å and $D = 2.38$ m ($\theta < 8°$). The sample and its blank were also measured without the container. The spectra recorded for the sample in the container and for the sample and container apart are reported in Fig. 3. The blank sample is a pure PSH solid sample. Its incoherent signal was measured in the same conditions as the

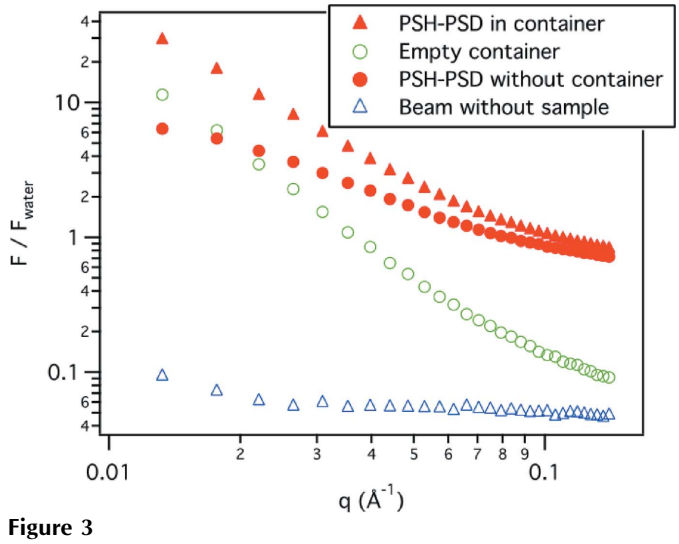

Figure 3
Ratio F/F_{water} of scattering functions of different samples to that of 1 mm-thick layer of water *versus* scattering vector q. Full triangles: 0.5 mm-thick solid sample made of 2% (*v*/*v*) deuterated polystyrene (PSD) and 98% (*v*/*v*) non-deuterated polystyrene (PSH) in a 3 mm-thick Al alloy container. Hollow circles: empty container. Full circles: solid sample alone. Hollow triangles: beam without sample. Measurements performed on PACE (LLB) at $\lambda = 6$ Å, $D = 2.38$ m. Statistical error bars are smaller than the data symbols.

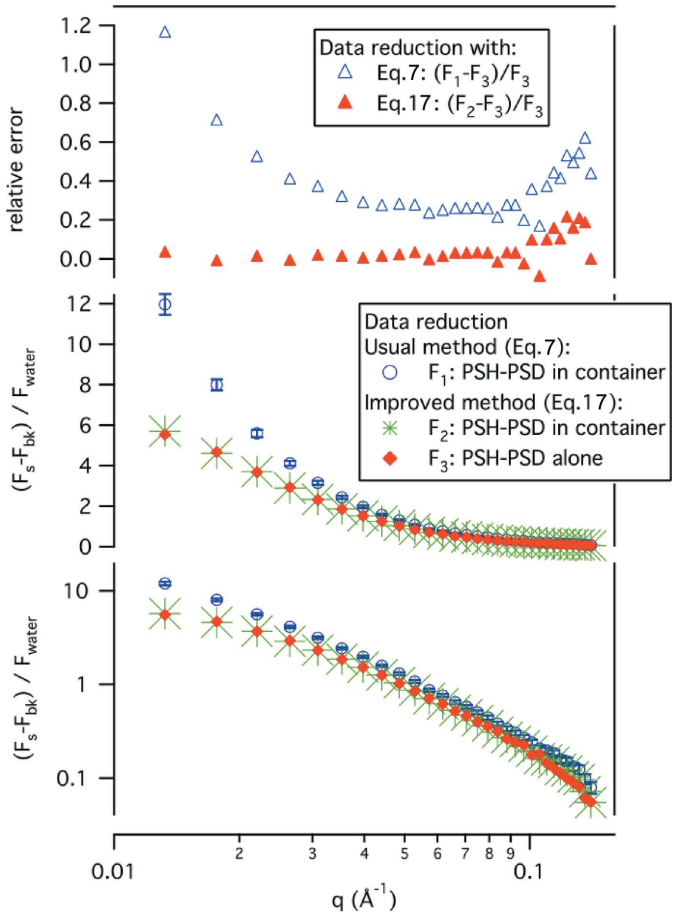

Figure 4
Comparison of the usual [equation (7)] and improved [equation (17)] data reduction methods for the measurements of Fig. 3. The reference spectrum is measured for the sample without container (F_3). For measurement of the same sample in a container that contributes to scattered intensity, the challenge for data treatment is to obtain a result as close as possible to the reference spectrum. This is achieved using equation (17) (F_2 superimposes to F_3) whereas the usual method fails [equation (7), F_1 does not superimpose to F_3].

sample and subtracted from the corresponding sample signals. Fig. 4 shows the data reduction (i) using all corrections [equation (17)] and (ii) using the usual approximation [equation (7)]. It appears that equation (17) allows us to account correctly for the container contribution and to superimpose scattering curves obtained for the sample alone and within the container. On the other hand, the usual data reduction method [equation (7)] leads to a huge overestimation of sample scattered intensity.

Note that our procedure for subtraction of the empty container contribution is valid whatever the origin of the scattering by the empty cell: coherent or incoherent. It is thus more general than the alternative procedure previously reported (Horkay *et al.*, 1991). In addition, our procedure is even valid for anisotropic scattering of the container, once isotropic averaging of the data has been performed. In the case of anisotropic scattering of the sample itself, the procedure remains equally valid but data treatment has to be performed without isotropic averaging.

2.4. Normalization of detector efficiency and absolute measurements

In order to account for different efficiencies of detector cells, normalization is achieved by dividing the signal of the sample by that measured with a reference sample giving a high flat signal (note that in this paper the term 'normalization' is always used with this meaning). Such a reference sample is generally a hydrogenated sample since the incoherent cross section of hydrogen is very high. The scattering function, $F_{\rm ref}(\theta)$, of this reference sample is obtained from the measured scattered intensity, $I_{\rm REF}$, once the 'beam without sample' and 'empty container' contributions have been adequately subtracted in the same way as for the sample [see equation (12)]:

$$F_{\rm ref}(\theta) = \frac{I_{\rm REF}(\theta) - B}{z_{\rm ref} T_{\rm REF} \alpha_{\rm REF}(\theta)} - \gamma_{\rm REF}(\theta) \frac{I_{\rm EC}(\theta) - B}{\beta_{\rm EC}(\theta) T_{\rm EC}} + \gamma_{\rm REF}(\theta) \left[\frac{T_{\rm EC}^{a(\theta)}}{\beta_{\rm EC}(\theta)} - \frac{T_{\rm REF}^{a(\theta)}}{\beta_{\rm REF}(\theta)} \right] F_{\rm b}(\theta). \quad (20)$$

Finally, to obtain the absolute values of the differential scattering cross sections (in $\rm cm^{-1}$) after data normalization, it is necessary to calculate

$$\tilde{\sigma}_{\rm s}(\theta) - \tilde{\sigma}_{\rm bk}(\theta) = \frac{\langle F_{\rm ref}(\theta) \rangle}{C(\lambda)} \times \frac{F_{\rm s}(\theta) - F_{\rm bk}(\theta)}{F_{\rm ref}(\theta)}, \quad (21)$$

where $C(\lambda)$ is the calibration constant [see equation (4)] and $\langle F_{\rm ref}(\theta) \rangle$ is the mean value of the incoherent scattering function used for normalization. To determine absolute values of the differential scattering cross section, different calibration methods can be equally used (Jacrot & Zaccaï, 1981; Wignall & Bates, 1987; Ragnetti *et al.*, 1985; Russell *et al.*, 1988; Cotton, 1991*b*; Glinka *et al.*, 1998; Lindner, 2002). Here, we only discuss the choice of the incoherent scatterer and the origin of deviations of the reference spectra from the expected flat profile, which are often observed.

2.4.1. Incoherent scatterer and multiple scattering. The reference sample can be an incoherent scatterer, such as highly hydrogenated samples. Among hydrogenated samples, a 1 mm-thick layer of water is a good choice. If experiments are performed in solutions of a hydrogenated solvent, the latter suits very well. A hydrogenated solid polymer such as poly(methylmethacrylate) or polycarbonate of about 1 mm thickness is also suitable, provided that its surfaces are not scratched (Ghosh & Rennie, 1999).

Once normalization is achieved, dimensionless spectra are obtained. The spectra then need to be multiplied by the cross section of the incoherent scatterer that has been chosen as reference sample [equation (21)]. Most of the hydrogenated reference samples used in SANS have a thickness close to the mean free path, Λ, of neutrons. However, their height and width are much larger ($\simeq 10\Lambda$). This means that neutrons scattered in these directions interact several times and have no chance to exit the sample at $\theta = 90°$. Their probability of going out forwards or backwards is thus increased (May *et al.*, 1982; Calmettes, 1999). This explains why the apparent cross

section of hydrogen can be found to be up to twice its nominal value of 80 barns.

In addition to this geometrical effect on the apparent cross section of the hydrogenated reference sample, it is important to emphasize the role of inelastic scattering that occurs at high q ($q > 1$ Å^{-1}) but adds to the forward signal as a result of multiple scattering. For such a reference sample, scattered neutrons reaching the detector display a wide distribution of wavelength. Thus, the measured count rate varies with the wavelength dependence of the detector efficiency [see equation (23) below].

As a major consequence, the apparent cross section of a given reference sample, *i.e.* the calibration factor, is a characteristic of each spectrometer. For instance, a difference of about 20% is observed at 5 Å between PACE (LLB) and D11 (ILL). Thus, calibration curves that have been published for specific spectrometers (May *et al.*, 1982; Ragnetti *et al.*, 1985) cannot be universal (Lindner, 2002).

2.4.2. Deviation of reference signal from a flat shape. In many cases, measured reference signals deviate from the expected flat profile and decrease at high q. The argument generally used to explain this observation is the multiple scattering that has been discussed in the previous section; the apparent cross section of the hydrogenated reference sample is increased in the forward direction and falls down at $\theta = 90°$. An angular dependence is thus expected and usually invoked to account for decreasing incoherent signals (Calmettes, 1999). In this section, we show that the decrease of the incoherent signal is properly accounted for using some simple geometrical arguments. Three contributions have to be considered:

(i) Angular dependence of the transmission [see equation (9) and Fig. 2] leads to a decrease of the measured intensity with θ.

(ii) Absence of curvature of the detector (Lindner *et al.*, 2000). The real solid angle of detector cell of area s is

$$\Delta\Omega(\theta) = \frac{s\cos\theta}{(D/\cos\theta)^2} = \Delta\Omega(0)\cos^3\theta. \qquad (22)$$

This leads to a decrease of the measured intensity with θ.

(iii) Detector efficiency ϵ depends on the actual thickness $z_0/\cos\theta$ of detection gas in the direction θ (Lindner *et al.*, 2000). This is expressed as

$$\epsilon(\lambda, \theta) = 1 - \exp[-\mu(\lambda)z_0/\cos\theta], \qquad (23)$$

where $\mu(\lambda)$ is the lineic absorption coefficient of the detection gas. It is a characteristic of the detector, proportional to the wavelength, and depends on the detection gas, pressure and thickness. For instance, $\mu(\lambda)z_0/\lambda = 0.20$ Å^{-1} on the PACE spectrometer at LLB. Equation (23) corresponds to an increase of detector efficiency with scattering angle.

Finally, for an incoherent signal which is normally independent of the scattering angle, the actual measured intensity varies as

$$I_{\rm ref}(\theta) = F_{\rm ref}(\theta)z_{\rm ref}T_{\rm ref}(\theta)\frac{\epsilon(\lambda, \theta)}{\epsilon(\lambda, 0)}\cos^3\theta. \qquad (24)$$

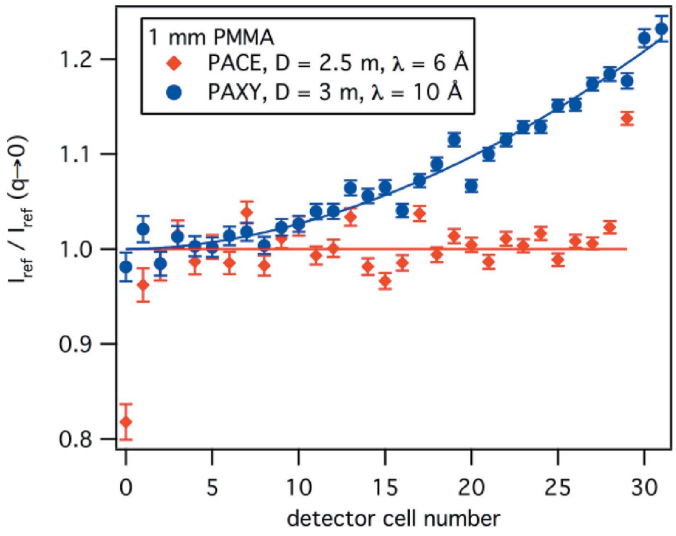

Figure 5
Scattered intensity of 1 mm-thick poly(methylmethacrylate) (PMMA) divided by the value at $q \to 0$ *versus* detector cell number (cell number 0 is the nearest to the beam). Circles: spectrometer PAXY, LLB (D = 3 m, λ = 10 Å). Diamonds: spectrometer PACE, LLB (D = 2.5 m, λ = 6 Å). In this q range geometrical effects due to $\cos\theta \neq 1$ can be neglected. The deviation from the expected flat profile is due to the gondola effect. Lines are guides for the eyes.

In order to check the validity of this expression, it is first necessary to take into account the 'gondola defect' often observed on multidetectors (Fig. 5). This is due to a regular increase of the thickness of the detection gas (BF_3 or He) from the center to the border of the detector (Lindner *et al.*, 2000). The gondola defect increases detector efficiency with scattering angle. It is observed on PAXY and PAXE at LLB, but it is not observed on our third spectrometer PACE. In practice, the gondola defect does not affect the shape of spectra as long as normalization is achieved using a reference sample measured using the same spectrometer configuration as for the sample. However, it has to be taken into consideration to test the validity of equation (24).

At small angles, the variation of $I_{\rm ref}(\theta)$ reported in equation (24) is negligible and measurements allow us to estimate the gondola effect. In Fig. 5, the scattered intensity of a sheet of poly(methylmethacrylate) measured on two spectrometers (PACE and PAXY at LLB) with a sample-to-detector distance $D \simeq 3$ m are compared. The deviation from a flat profile is due to the gondola effect. PACE is free from this defect and is used in the next section to test equation (24).

In Fig. 6, the incoherent signal of a water layer of 1 mm thickness is compared with equation (24) with the zero q scattered intensity as the only adjustable parameter. One can see that equation (24) fully accounts for the decrease of $I_{\rm ref}(\theta)$. As a consequence, for a given configuration (D, λ) of the spectrometer, a hydrogenated sample is suitable for normalization of measurements following equation (21), at least up to q values of 0.7 Å^{-1}, the upper limit of our SANS experiments.

2.4.3. Fast measurement of reference signal. Frequently, scattered intensity is measured at different detector positions, D, and wavelengths, λ. Then, superimposition of data obtained

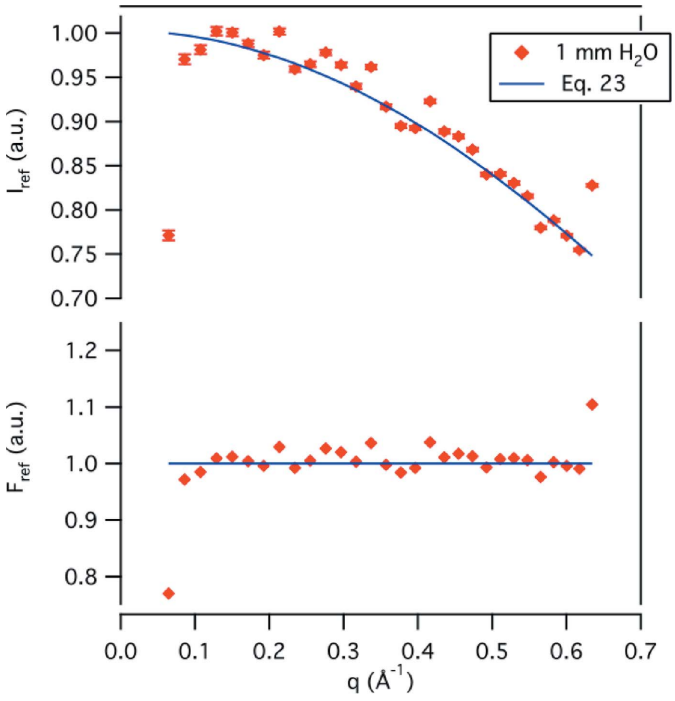

Figure 6
Top: raw incoherent signal, $I_{\rm ref}(\theta)$, of 1 mm of H_2O measured on the spectrometer PACE at high q (D = 0.65 m; λ = 4.5 Å). The full line is equation (24) with $I_{q\to 0}$ as the only adjustable parameter. Bottom: incoherent scattering function, $F_{\rm ref}(\theta) = I_{\rm ref}(\theta)/\left[T(\theta)\epsilon(\lambda,\theta)\cos^3\theta\right]$. The expected flat profile is recovered. Note that even the first and last points of the spectrum, which show a large deviation from the curve due to the beam stop and edges of the detector, are finally accounted for after the last stage [equation (21)] of data treatment (see for instance Fig. 4).

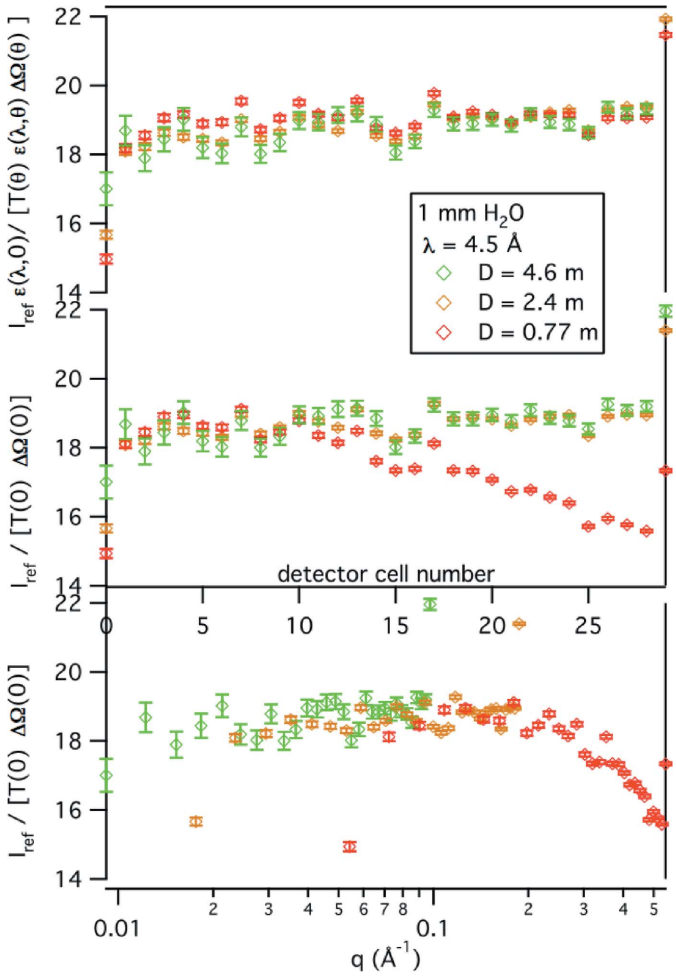

Figure 7
Scattered intensity, $F_{\rm ref}$, of a 1 mm-thick layer of water in a quartz container measured on PACE at LLB at $\lambda = 4.5$ Å and three different distances, D, between sample and detector. Bottom and middle: $F_{\rm ref} = I_{\rm ref}/[T(0)\Delta\Omega(0)]$ *versus* scattering vector q or detector cell number. The $F_{\rm ref}$ so calculated corresponds to the approximation $\cos\theta = 1$. Data measured at high q display a different profile. Top: $F_{\rm ref} = I_{\rm ref}\epsilon(\lambda,0)/[T(\theta)\epsilon(\lambda,\theta)\Delta\Omega(\theta)]$ calculated following equation (24). The three spectra superimpose well.

under different configurations requires normalization measurements and absolute calibrations for each configuration. At large distances and large wavelengths, measurements require a long time to obtain good statistics. Actually, (i) the incoherent count rate scales as the solid angle $1/D^2$, (ii) an appropriate symmetric collimation of neutron beam decreases the flux by the same factor, $1/D^2$, and (iii) the neutron flux through a mechanical selector decreases roughly as $1/\lambda^4$. Therefore, at small angle $q \propto (\lambda D)^{-1}$, the time needed to measure the flat scattering of an incoherent sample decreases as q^{-4}. Good normalization measurements at low q would require a huge amount of beam time. However, equation (24) can be used to improve the statistics and save time. Actually, only measurement of the incoherent signal at a short distance (with the same wavelength and beam collimation) is needed. Equation (24) allows us to calculate the normalization spectrum that has to be used for reduction of data obtained at smaller q. For instance, if normalization measurement is performed at $D = 1$ m instead of $D = 5$ m, the corresponding beam time is reduced by 25, *i.e.* the ratio of solid angles.

This method gives very good results, as shown in Fig. 7, which reports measurements of scattered intensity of a 1 mm thick layer of water in a quartz container. Measurements are performed at $\lambda = 4.5$Å and $D = 0.76$, 2.38 and 4.6 m, respectively. Beam collimation is ensured by two diaphragms ($\phi = 7$ and 12 mm) separated by 2.5 m for the two smallest distances and by 5 m for the highest one. For this reason, data obtained at $D = 4.6$ m are multiplied by a factor 4 to account for the corresponding beam flux. In Fig. 7, once angular corrections of equation (24) are taken into account, the three spectra superimpose within 2% error bars (even detector defects are reproduced). Such a difference is weak compared with the other errors for absolute calibration.

3. Determination of the inherent sample background

Another problem of SANS data reduction is concerned with the proper subtraction of the inherent sample background. In the following, we first recall the expression for the scattering cross section of a sample (§3.1). Then, we discuss the choice of an ideal blank sample and explain how to determine the inherent sample background from the scattering of an actual blank sample (§3.2).

3.1. Expression of the scattering cross section of a sample

Let us consider a generalized solution of volume V made of different chemical species. $\alpha = 1$ denotes the solvent and $\alpha = 2m$ the different solutes. For each component, v_α is the partial molar volume, a_α the coherent scattering length, $b_\alpha = a_\alpha - a_1 v_\alpha / v_1$ the contrast length ($b_1 = 0$), and $x_\alpha = n_\alpha v_\alpha / V$ the volume fraction occupied by the n_α molecules. The coherent scattering cross section per volume and solid angle units, $\tilde{\sigma}(q)$, is expressed as a function of concentration and density fluctuations as (Cotton, 1991*a*)

$$\begin{aligned}\tilde{\sigma}(q < q^*) &= (1/V) \sum_{\alpha,\beta} b_\alpha b_\beta S_{\alpha\beta}(q) + A_\mathrm{s} kT \chi_T^\mathrm{s} \\ &= s(q) + A_\mathrm{s} kT \chi_T^\mathrm{s}. \end{aligned} \tag{25}$$

$s(q)$ is the coherent scattering cross section of concentration fluctuations and is the interesting quantity. χ_T^s is the isothermal compressibility of the solution and q^* the reverse correlation length of density fluctuations (Cotton, 1991*b*). In practice, $q^* > 0.5$ Å^{-1}. The contribution of compressibility to the coherent scattered intensity is weighted by the contrast factor A_s:

$$A_\mathrm{s} = \frac{a_1}{v_1} \sum_1^m \frac{x_\alpha}{v_\alpha} (b_\alpha + a_\alpha). \tag{26}$$

As $x_1 = 1 - \sum_{\alpha=2}^m x_\alpha$, A_s can be rewritten as

$$A_\mathrm{s} = A_1 \left(1 + 2 \frac{v_1}{a_1} \sum_2^m x_\alpha \frac{b_\alpha}{v_\alpha} \right) \quad \text{with} \quad A_1 = \frac{a_1^2}{v_1^2}. \tag{27}$$

Assuming that the partial molar volume of pure solvent remains unaffected with solute addition, A_s is simply expressed as a function of solvent characteristics A_1.

For neutrons, scattering depends on the isotope and on the spin state of the nucleus. The corresponding fluctuations cause an additional contribution to the scattering cross section: $V\tilde{\sigma}^\mathrm{inc}$. If $a_i^\mathrm{inc} = (\langle a_i^2 \rangle - \langle a_i \rangle^2)^{1/2}$ is the incoherent scattering length of the ith nucleus of scatterer α (with $i = 1 N_\alpha$), the incoherent scattering cross section, $\tilde{\sigma}^\mathrm{inc}$, of the solution can be written as

$$\begin{aligned}\tilde{\sigma}_\mathrm{s}^\mathrm{inc} &= (1/V) \sum_{\alpha=1}^m n_\alpha \left[\sum_{i=1}^{N_\alpha} \left(a_i^\mathrm{inc} \right)^2 \right] \\ &= \sum_{\alpha=1}^m (x_\alpha / v_\alpha) \left[\sum_{i=1}^{N_\alpha} \left(a_i^\mathrm{inc} \right)^2 \right] = \sum_{\alpha=1}^m \tilde{\sigma}_\alpha^\mathrm{inc}, \end{aligned} \tag{28}$$

where $\tilde{\sigma}_\alpha^\mathrm{inc}$ is the incoherent scattering cross section per solid angle and per volume unit of species α. Finally, the total scattering cross section per solid angle and per volume unit is

$$\begin{aligned}\tilde{\sigma}_\mathrm{s}(q) &= \tilde{\sigma}(q) + \tilde{\sigma}_\mathrm{s}^\mathrm{inc} \\ &= s(q) + A_\mathrm{s} kT \chi_T^\mathrm{s} + \tilde{\sigma}_\mathrm{s}^\mathrm{inc}. \end{aligned} \tag{29}$$

It is deduced from the measurement of scattering intensity following equation (4). Nevertheless, $s(q)$ is the meaningful function for the sample structure [see equation (25)] and the problem is to evaluate the q-independent terms of equation (29), *i.e.* the inherent sample background:

$$\tilde{\sigma}_\mathrm{sbkg} = A_\mathrm{s} kT \chi_T^\mathrm{s} + \tilde{\sigma}_\mathrm{s}^\mathrm{inc}. \tag{30}$$

This is achieved by measuring the scattered intensity of a blank sample.

3.2. Choice of a blank sample

An ideal blank sample would display a scattering cross section, $\tilde{\sigma}_\mathrm{bk}$, independent of q, such as

$$\tilde{\sigma}_\mathrm{sbkg} = \tilde{\sigma}_\mathrm{bk} = A_\mathrm{bk} kT \chi_T^\mathrm{bk} + \tilde{\sigma}_\mathrm{bk}^\mathrm{inc}. \tag{31}$$

In principle, a blank sample having the same incoherent scattering cross section as the sample to be studied can be easily prepared. However, the contrast weighting coefficient of density fluctuations will probably differ. Comparing density fluctuations and incoherent scattering contributions with the scattered intensity for simple cases (see Appendix *B*), it appears that χ_T^s and χ_T^bk can both be neglected for solutions in hydrogenated solvents. For instance, the ratio $\tilde{\sigma}_\mathrm{bk}^\mathrm{inc} / (A_\mathrm{bk} kT \chi_T^\mathrm{bk}) \simeq 7300$ for H_2O. However, for a deuterated solvent, compressibility has to be taken into account: $\tilde{\sigma}_\mathrm{bk}^\mathrm{inc} / (A_\mathrm{bk} kT \chi_T^\mathrm{bk}) \simeq 1.4$ for D_2O. These two cases are discussed in the next sections.

3.2.1. Incoherent scattering predominates. In this case, the sample inherent background can be reasonably estimated by

$$\tilde{\sigma}_\mathrm{sbkg} \simeq \tilde{\sigma}_\mathrm{s}^\mathrm{inc}. \tag{32}$$

A first approximation would be to use the pure solvent as blank sample. Its incoherent intensity, $\tilde{\sigma}_\mathrm{bk}^\mathrm{inc}$, however, differs from that of the sample, $\tilde{\sigma}_\mathrm{s}^\mathrm{inc}$, owing to the solute. Nevertheless, knowing the sample composition and the volume fraction of solute, it is possible from tables (Sears, 1992) to calculate the ratio $\left(\tilde{\sigma}_\mathrm{s}^\mathrm{inc} / \tilde{\sigma}_\mathrm{bk}^\mathrm{inc} \right)_\mathrm{calc}$ of the expected scattering cross sections. Then, the actual incoherent scattering cross section of the sample could be estimated by

$$\tilde{\sigma}_\mathrm{s}^\mathrm{inc} \simeq \tilde{\sigma}_\mathrm{bk}^\mathrm{inc} \left(\tilde{\sigma}_\mathrm{s}^\mathrm{inc} / \tilde{\sigma}_\mathrm{bk}^\mathrm{inc} \right)_\mathrm{calc}, \tag{33}$$

where $\tilde{\sigma}_\mathrm{bk}^\mathrm{inc}$ is the measured incoherent scattering cross section of the solvent (see Appendix *B*). Unfortunately, this is not valid because multiple scattering (Calmettes, 1999; Strunz *et al.*, 2000) causes the measured intensity to be much higher than and not proportional to the calculated intensity (see §2.4.1). Note that this problem cannot be bypassed by decreasing the sample thickness as the effect is due to the sample size in the directions perpendicular to the neutron beam.

More properly, a blank sample has to be prepared using a mixture of deuterated and non-deuterated solvent. Assuming that deuteration does not change the partial molar volume, the volume fraction x_slvD of deuterated solvent in this blank sample needs to fulfill the condition

$$\begin{aligned}\tilde{\sigma}_\mathrm{s}^\mathrm{inc} = \tilde{\sigma}_\mathrm{bk}^\mathrm{inc} = (1/v_1) \Big[& x_\mathrm{slvD} \left(a_\mathrm{slvD}^\mathrm{inc} \right)^2 + (1 - x_\mathrm{slvD}) \left(a_\mathrm{slvH}^\mathrm{inc} \right)^2 \\ & + x_\mathrm{slvD} (1 - x_\mathrm{slvD}) (a_\mathrm{slvD} - a_\mathrm{slvH})^2 \Big], \end{aligned} \tag{34}$$

with $\tilde{\sigma}_\mathrm{s}^\mathrm{inc}$ calculated following equation (28).

Table 1
Examples of different contributions in the inherent background of a solution.

c is the solute concentration. Subscripts 1, 2 and s refer to solvent, solute and solution, respectively. $\tilde{\sigma}$ is a differential cross section per volume unit. $x_{\rm slvD}$ is the fraction of deuterated solvent in a blank composed of H and D solvent with the same incoherent scattering cross section as the sample. $A_1 kT\chi_T^1$, $A_x kT\chi_T^1$ and $A_s kT\chi_T^1$ are the compressibility contributions to scattered intensity of pure solvent, of a blank with a fraction $x_{\rm slvD}$ of deuterated solvent and of the sample, respectively. $\tilde{\sigma}_{\rm s}^{\rm inc}$ is the incoherent contribution to the inherent background of the sample. $\mathrm{Err}_1 = (\tilde{\sigma}_{\rm bk1} - \tilde{\sigma}_{\rm sbkg})/\tilde{\sigma}_{\rm sbkg}$ is the error using the pure solvent as blank. $\mathrm{Err}_2 = (\tilde{\sigma}_{\rm bk2} - \tilde{\sigma}_{\rm sbkg})/\tilde{\sigma}_{\rm sbkg}$ is the error using a blank with a fraction $x_{\rm slvD}$ of deuterated solvent. Negative values correspond to underestimations and positive values to overestimations.

Solution	c (10^{-2} g cm^{-3})	$\tilde{\sigma}_1^{\rm inc}$ (10^{-2} cm^{-1})	$\tilde{\sigma}_2^{\rm inc}$ (10^{-2} cm^{-1})	$x_{\rm slvD}$ (%)	$A_1 kT\chi_T^1$ (10^{-2} cm^{-1})	$A_x kT\chi_T^1$ (10^{-2} cm^{-1})	$A_s kT\chi_T^1$ (10^{-2} cm^{-1})	$\tilde{\sigma}_{\rm s}^{\rm inc}$ (10^{-2} cm^{-1})	Err_1 (%)	Err_2 (%)
PSH/C_6D_6	10	0.611	2.95	94.2	1.164	1.052	**0.990**	**3.564**	−60	−1.4
	1	0.658	0.295	99.4	1.164	1.115	**1.148**	**0. 953**	−13	0.28
C_6D_6†							**1.164**	**0.668**		
PSD/C_6H_6	10	24.3	0.079	28.2	0.0554	0.211	**0.102**	**24.33**	6.3	−0.45
	1	25.9	0.0079	10.6	0.0554	0.103	**0.060**	**25.94**	−0.17	−0.16
C_6H_6†							**0.055**	**25.9**		
PSD/CS_2	10	0.00110	0.070		0.057		**0.101**	**0.071**	−66	
	1	0.00180	0.0070		0.057		**0.061**	**0.008**	−16	
CS_2†							**0.057**	**0.001**		

† Values from Table 2.

A blank sample so prepared, measured with the same wavelength and container geometry, displays the same transmission and the same multiple scattering as the sample. The incoherent signal so measured can be adequately subtracted from the scattered intensity of the sample. At this point, one may question why the sample and the blank have the same transmissions while the sample displays an additional important central scattering. Actually, transmission takes into account the integral over 4π steradians of incoherent and coherent scattering. The coherent contribution is negligible for the blank (this section is precisely concerned with this case), while it is concentrated in a few 10^{-3} steradians for the sample. The latter integral is often negligible compared with the incoherent contribution.

As an example, for a solution at 0.1 g cm^{-3} of D-polystyrene in H-benzene, the proper blank contains 28% (volume fraction) of D-benzene (see Appendix *B*). This high volume fraction is a result of the composition fluctuations term, *i.e.* the last term in equation (34). Note that possible isotopic exchange in solvent mixtures (as in H_2O/D_2O mixtures) results in a still higher incoherent background, since the solvent mixture contains more than two components (see Appendix *B*).

Sometimes, because of inaccuracy of volume or weight measurements, a blank sample prepared following equation (34) does not display exactly the same transmission as the sample. Then a good approximation consists of multiplying the blank spectrum by the ratio of the logarithm of blank transmission to that of sample transmission.

3.2.2. Incoherent scattering does not predominate. In this case, exact calculation of the inherent sample background following equation (30) is not easy because χ_T^1 is known for pure solvents (see Appendix *B*), but $\chi_T^{\rm s}$ is generally unknown for solutions. A reasonable approximation assumes $\chi_T^{\rm s} \simeq \chi_T^1$. Then, equation (30) becomes

$$\tilde{\sigma}_{\rm sbkg} \simeq A_{\rm s} kT\chi_T^1 + \tilde{\sigma}_{\rm s}^{\rm inc} \qquad (35)$$

where $A_{\rm s}$ and $\tilde{\sigma}_{\rm s}^{\rm inc}$ can be calculated following equations (27) and (28), respectively. Examples are reported in Table 1. In this table, our better estimation of $\tilde{\sigma}_{\rm sbkg}$ given by equation (35) is used to compare the accuracy of the usual approximations that consist of (i) using the pure solvent as blank: $\tilde{\sigma}_{\rm bk1} = A_1 kT\chi_T^1 + \tilde{\sigma}_1^{\rm inc}$; (ii) using a blank made of H and D solvent with the same incoherent scattering cross section as the sample: $\tilde{\sigma}_{\rm bk2} = A_x kT\chi_T^1 + \tilde{\sigma}_{\rm s}^{\rm inc}$.

The consequences of such errors are especially important at high q where coherent scattering is generally weak.

A proper blank sample would be a mixture of H and D solvents obtained by a calculation similar to that described in the previous section [see equation (34)] but accounting for the difference in compressibility terms. Such a blank sample would now fulfill the condition

$$\tilde{\sigma}_{\rm sbkg} = A_{\rm bk} kT\chi_T^1 + \tilde{\sigma}_{\rm bk}^{\rm inc} \qquad (36)$$

with

$$A_{\rm bk} = A_1\left[1 + 2x_{\rm slvD}\left(\frac{a_{\rm slvD}}{a_{\rm slvH}} - 1\right)\right]$$

and

$$\tilde{\sigma}_{\rm bk}^{\rm inc} = \frac{1}{v_1}\Big[x_{\rm slvD}\big(a_{\rm slvD}^{\rm inc}\big)^2 + (1 - x_{\rm slvD})\big(a_{\rm slvH}^{\rm inc}\big)^2 + x_{\rm slvD}(1 - x_{\rm slvD})(a_{\rm slvD} - a_{\rm slvH})^2\Big],$$

with $\tilde{\sigma}_{\rm sbkg}$ calculated following equation (35). In equation (36), the only unknown quantity is $x_{\rm slvD}$ and, in principle, a blank could be prepared solving this equation. However, in practice, this would be tedious, particularly in the case of a long series of different samples.

3.3. Systematic methods for inherent background calibration

During a long series of measurements with similar samples, it is possible to reduce the beam time devoted to determination of inherent backgrounds by making a calibration curve of the background level. As stressed above, measurements on

samples and blanks have to be performed in conditions leading to the same multiple scattering effect, *i.e.* with same wavelength and same thickness. Here again, two cases have to be considered depending on the incoherent background.

3.3.1. Calibration for high incoherent background. This is the case of a hydrogenated matrix (solids or solutions). The method involves measuring scattering intensities of a series of blanks composed of H and D solvents, varying the volume fraction of D solvent in a range of concentration such that the blank transmissions cover those of the samples. As flat signals are expected for these blanks, the statistics are increased by averaging each spectrum over q. Then, an accurate reference curve, $\mathcal{C}_\infty$, of the level of the incoherent signal as a function of the transmission, $T_{\rm bk}$, is experimentally determined:

$$\tilde{\sigma}_{\rm bk} \simeq \tilde{\sigma}_{\rm bk}^{\rm inc} = \mathcal{C}_1(T_{\rm bk}). \tag{37}$$

The inherent background of the sample is then determined from the value of its transmission as equal to $\tilde{\sigma}_{\rm sbkg} \simeq \tilde{\sigma}_{\rm s}^{\rm inc} = \mathcal{C}_1(T_{\rm s})$.

Note that the use of transmission as a characteristic for the incoherent scattering is valid if absorptions of samples and solvent mixtures are negligible. This is the case of most organic solvents.

3.3.2. Calibration for a series of solid samples. For a series of solid samples, some difficulties may arise from the control of sample thicknesses or inaccuracy in their measurements (for instance due to sample roughness or mechanical stress).

For such a series with a given amount of incoherent scatterers, both the incoherent scattering and the sample transmission depend unambiguously on the sample thickness. Thus, two calibration curves can be obtained from the measurement of a few blank samples having different well controlled thicknesses.

$$\begin{aligned} \tilde{\sigma}_{\rm bk} \simeq \tilde{\sigma}_{\rm bk}^{\rm inc} &= \mathcal{C}_2(T_{\rm bk}), \\ z_{\rm bk} &= \mathcal{C}_3(T_{\rm bk}). \end{aligned} \tag{38}$$

The first calibration curve is identical to equation (37), whereas the second aims to provide the sample thickness from its transmission: $z_{\rm s} = \mathcal{C}_3(T_{\rm s})$.

For instance, this method has been used for the study of the relaxation of conformation of stretched solid polymers (Fourmaux-Demanges, 1998). Samples were made of a mixture of 50% of D-labelled polymers (with only 17% of protons replaced by deuterium) and 50% of H polymers (without deuterium) in order to access the single chain form factor. In this case, for the different thicknesses needed for the calibration curve, $\tilde{\sigma}_{\rm bk}$ is calculated as equal to the half sum of the scattering intensities delivered by a 100% H polymer sample and a 100% D-labelled polymer sample.

Note that in the case of solid blank samples surface roughness may be responsible for small-angle scattering. Thus, the scattering cross section $\tilde{\sigma}_{\rm bk}$ that has to be accepted for the calibration curve corresponds to the high q limit of the spectrum.

3.3.3. Calibration for weak incoherent background. In this case, the role of density fluctuations in the scattered intensity of a blank sample cannot be neglected. As these fluctuations mainly contribute to high q signals (for instance the first-neighbor correlation peak in liquids), transmission of the sample does not reflect scattered intensity measured at low q (for instance an increase of the signal at high q should be responsible for a decrease of transmission but would probably have no effect on scattered intensity at low q). The transmission value is not a characteristic of the background level.

From equation (36), it appears that for the blank this characteristic can be more adequately taken as the volume fraction, $x_{\rm bk}^{\rm inc}$, of incoherent scatterers (the minority species):

$$\tilde{\sigma}_{\rm bk} = A_{\rm bk} kT \chi_T^1 + \tilde{\sigma}_{\rm bk}^{\rm inc} = \mathcal{C}_4(x_{\rm bk}^{\rm inc}). \tag{39}$$

The reference curve $\mathcal{C}_4(x_{\rm inc})$ is obtained by preparing different blanks varying $x_{\rm bk}^{\rm inc}$. For a given sample, an ideal blank composition, $x_{\rm s}^{\rm inc}$, can be calculated following equation (36). The inherent background of this sample is thus approximated as equal to $\mathcal{C}_4(x_{\rm s}^{\rm inc})$ and deduced from the reference curve.

4. Conclusion

This paper provides a survey of problems for background subtraction in SANS experiments.

Our first discussion is devoted to data obtained at scattering angles above 10° where $\cos\theta$ differs significantly from 1. Angular corrections play a role in transmission values and in the efficiency of the detector. For instance, the decrease of the scattering intensity of water at large angles is shown to be due to a geometrical effect that can be easily corrected. This result suggests a method for measuring quickly the reference scattering needed for normalization of cells of the position-sensitive detector when it is far from the sample and the neutron count rate is too weak.

Secondly, we discuss the case of a sample container that gives spurious scattering. The proper method allowing subtraction of this contribution to sample scattering is given and has been experimentally verified. Note that the correct subtraction method requires measurements of both 'empty container' and 'beam without sample' scattering. As a result, it is possible to use containers with strongest windows which are useful for studies of samples under high pressures, very low or very high temperatures, and under stress.

Thirdly, subtraction of the inherent sample background is considered. Two complications arise. The first is multiple scattering that occurs with incoherent scatterers. It comes from the geometry of the sample containers used to maximize the neutron flux. It is difficult to calculate, so we only give methods allowing for the preparation of blank samples delivering the same multiple scattering as that of the sample. The second complication is the contribution of compressibility. We give an expression allowing the evaluation of this coherent background. It is often negligible but involves contrast terms that may reveal important surprises.

Even if the corrections proposed here are somewhat tedious, it seems reasonable to increase the accuracy of SANS measurements by introducing them systematically in data treatment procedures.

Throughout this paper it is assumed that the different contributions for background subtraction add to one another. For example, the contribution from the empty container adds to that from the sample, or incoherent scattering adds to coherent scattering. Implicitly this is only valid for single scattering. As soon as multiple scattering is not negligible, these different contributions do not simply add but are convoluted with each other component, making background subtraction more complicated. To our knowledge, this is still an unsolved problem. Generally, multiple scattering involves highly scattered intensity that renders background subtraction a secondary problem. In the case of negligible background, the effects of multiple scattering can be removed from the data (Schelten & Schmatz, 1980; Monkenbusch, 1991) so as to obtain the coherent, single scattering cross section of the sample.

Finally, prior to data analysis, a last stage for data treatment is sometimes necessary. It consists of signal desmearing (Glatter, 1977) that accounts for the resolution function. For this stage, the q-dependent resolution of the spectrometer has to be calculated (Pedersen *et al.*, 1990; Lairez, 1999). The latter calculation is also implemented in the new software for data treatment at LLB (Lairez, 2006).

APPENDIX *A*
Scattering by a sample inside a container

The problem of scattering by a sample inside a container is slightly complicated by a possible contribution of the container (aluminium sheets, alloy windows *etc.*). This problem can be solved if multiple scattering is negligible. Let us consider a sample of thickness z_s between two windows of the same thickness, z_{ec}, and made with the same material (see Fig. 8). The scattering intensity is the sum of three components that depend on the location of interaction between the neutron and the scatterer. Scattering functions are denoted $F_{ec}(\theta)$ for the front and back windows of the container and $F_s(\theta)$ for the sample.

The scattered intensities can be written as

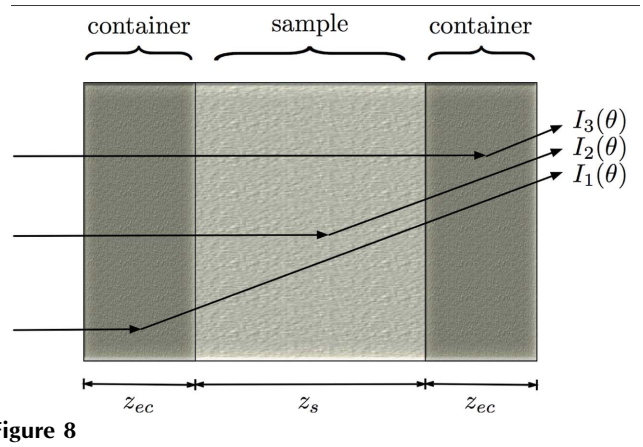

Figure 8
Schematic representation of the scattering by a sample of thickness z_s in a container with front and back windows of thicknesses z_{ec1} and z_{ec2}, respectively.

$$I_1(\theta) = \int_0^{z_{ec}} \mathrm{d}x \exp[-\mu_{ec}x]\, F_{ec}(\theta) \exp[-\mu_s(z_s - x)/\cos\theta] \times \exp[-(\mu_s z_s + \mu_{ec} z_{ec})/\cos\theta], \quad (40)$$

$$I_2(\theta) = \int_0^{z_s} \mathrm{d}x \exp[-(\mu_{ec} z_{ec} + \mu_s x)]\, F_s(\theta) \times \exp[-\mu_s(z_s - x)/\cos\theta] \exp(-\mu_{ec} z_{ec}/\cos\theta), \quad (41)$$

$$I_3(\theta) = \int_0^{z_{ec}} \mathrm{d}x \exp(-\mu_{ec}x)\, F_{ec}(\theta) \exp[-\mu_{ec}(z_{ec} - x)/\cos\theta] \times \exp[-(\mu_s z_s + \mu_{ec} z_{ec})]. \quad (42)$$

The total intensity is the sum of $I_1(\theta)$, $I_2(\theta)$ and $I_3(\theta)$. Let us define the following quantities:

$$T_i = \exp(-\mu_i z_i),$$

$$T_i(\theta) = T_i \frac{1 - T_i^a(\theta)}{a(\theta)\mu_i},$$

$$a(\theta) = (1/\cos\theta) - 1$$

$$T_i^\theta = T_i^{1/\cos\theta}.$$

Note that the transmission, T_S, measured for the sample inside its container is related to the transmissions of each layer of the overall sample by

$$T_S = T_{ec}^2 T_s = T_{EC} T_s = \exp[-(2\mu_{ec} z_{ec} + \mu_s z_s)].$$

Uppercase subscript S refers to the sample inside the container and uppercase subscript EC to the overall empty container, whereas lowercase subscripts s and ec stand for the sample alone and the two windows of the container.

During the experiment, the scattering signal $I_S(\theta)$ recorded on the detector is

$$\begin{aligned} I_S(\theta) = {} & T_s(\theta) T_{ec} T_{ec}^\theta F_s(\theta) \\ & + T_{ec}(\theta)\left(T_{ec}^\theta T_s^\theta + T_{ec} T_s\right) F_{ec}(\theta) \\ & + \left(T_{ec}^\theta\right)^2 T_s^\theta F_b(\theta) + B. \end{aligned}$$

That of the empty container is

$$I_{EC}(\theta) = T_{ec}(\theta)\left(T_{ec}^\theta + T_{ec}\right) F_{ec}(\theta) + \left(T_{ec}^\theta\right)^2 F_b(\theta) + B.$$

In this formula, we can check that the scattering intensity of the empty container is weighted by the usual factor:

$$\begin{aligned} T_{ec}(\theta)(T_{ec}^\theta + T_{ec}) &= T_{ec} \frac{1 - T_{ec}^{a(\theta)}}{a(\theta)\mu_{ec}} \left\{ T_{ec}\left[1 + T_{ec}^{a(\theta)}\right] \right\} \\ &= T_{ec}^2 \frac{1 - T_{ec}^{2a(\theta)}}{a(\theta)\mu_{ec}} \\ &= T_{EC}(\theta). \end{aligned}$$

It is useful to write all coefficients as a function of experimental parameters T_S, T_{EC}, z_s and z_{ec}. The equations

Table 2
Numerical value for simple scatterers.

v is the molecular volume; a is the coherent scattering length; a^{inc} is the incoherent scattering length (Sears, 1992); χ_T is the isothermal compressibility at 298 K (Lide, 1995–1996; Brandrup & Immergut, 1989); $\tilde{\sigma}_{inc}$ is the incoherent scattering cross section per volume and solid angle unit. CS_2 is an interesting and rare solvent with a very low incoherent scattering cross section.

Scatterer		v^{-1} (10^{21} cm^{-3})	a (10^{-12} cm)	$(a^{inc})^2$ (10^{-24} cm^2)	$kT\chi_T$ (10^{-24} cm^3)	$a^2v^{-2}kT\chi_T$ (10^{-2} cm^{-1})	$\tilde{\sigma}^{inc}$ (10^{-2} cm^{-1})
Water	H_2O	33.4	−0.167	12.8	1.88	**0.00587**	**42.7**
Heavy water	D_2O	33.4	1.92	0.327	1.88	**0.772**	**1.09**
H-cyclohexane	C_6H_{12}	5.58	−0.500	76.6	4.69	**0.00365**	**42.5**
D-cyclohexane	C_6D_{12}	5.58	12.0	1.96	4.69	**2.10**	**1.09**
H-benzene	C_6H_6	6.77	1.74	38.3	3.98	**0.0554**	**25.9**
D-benzene	C_6D_6	6.77	7.99	0.981	3.98	**1.16**	**0.668**
Carbon disulfide	CS_2	10.0	1.23	0.00120	3.79	**0.0577**	**0.00120**
H-polystyrene	$-(C_8H_8)_n-$	6.15	2.33	51.1	0.910	**0.0186**	**31.4**
D-polystyrene	$-(C_8D_8)_n-$	6.15	10.7	1.31	0.910	**0.391**	**0.805**

$$
\begin{aligned}
T_s(\theta)T_{ec}T_{ec}^{\theta} &= z_s T_S\left[T_{EC}^{a(\theta)/2}\,\frac{1-(T_S/T_{EC})^{a(\theta)}}{-a(\theta)\ln(T_S/T_{EC})}\right]\\
&= z_s T_S\,\alpha_S(\theta),\\
T_{ec}(\theta)(T_{ec}^{\theta}T_s^{\theta}+T_{ec}T_s) &= 2z_{ec}T_S\\
&\quad\times\frac{1-T_{EC}^{a(\theta)/2}}{-a(\theta)\ln(T_{EC})}\left[1+\left(\frac{T_S}{T_{EC}^{1/2}}\right)^{a(\theta)}\right]\\
&= 2z_{ec}T_S\,\beta_S(\theta),
\end{aligned}
$$

introduce $\alpha_S(\theta)$ and $\beta_S(\theta)$. Finally, we obtain for the scattered intensity of the sample

$$I_S(\theta) = z_s T_S\alpha_S(\theta)F_s(\theta) + 2z_{ec}T_S\beta_S(\theta)F_{ec}(\theta) + T_S^{\theta}F_b(\theta) + B,$$

and for the empty container

$$I_{EC}(\theta) = 2z_{ec}T_{EC}\beta_{EC}(\theta)F_{ec}(\theta) + T_{EC}^{\theta}F_b(\theta) + B.$$

As a result, the scattering function of the sample $F_s(\theta)$ is

$$
\begin{aligned}
F_S(\theta) = {}& \frac{I_S(\theta)-B}{z_s T_S\alpha_S(\theta)} - \frac{\beta_S(\theta)}{z_s\alpha_S(\theta)}\left[\frac{I_{EC}(\theta)-B}{\beta_{EC}(\theta)T_{EC}}\right]\\
&+\frac{1}{z_s\alpha_S(\theta)}\left[\frac{\beta_S(\theta)T_{EC}^{\theta}}{\beta_{EC}(\theta)T_{EC}} - \frac{T_S^{\theta}}{T_S}\right]F_b(\theta)
\end{aligned}
$$

Finally, this reduces to equation (12).

APPENDIX *B*
Incoherent scattering of an H and D solvent mixture: example of calculation

Let us consider a hydrogenated solvent of molar mass m_{slvH} and volumic mass ρ_H. It contains $1/v_{solv} = \mathcal{N}_a\rho_H m_{slvH}$ molecules per volume unit, where $\mathcal{N}_a$ is Avogadro's number. The coherent and incoherent scattering lengths are a_{slvH} and a^{inc}_{slvH}. Its deuterated homolog is assumed to have the same partial molar volume and to be characterized by a_{slvD} and a^{inc}_{slvD}. For a mixture made of a fraction x_{slvD} of D molecules and a fraction $(1-x_{slvD})$ of H molecules, the incoherent scattering per solid angle and volume unit is

$$
\begin{aligned}
\tilde{\sigma}^{inc}_{solv} = (1/v_{solv})\Big[&x_{slvD}(a^{inc}_{slvD})^2 + (1-x_{slvD})(a^{inc}_{slvH})^2\\
&+ x_{slvD}(1-x_{slvD})(a_{slvD}-a_{slvH})^2\Big].
\end{aligned}
\tag{43}
$$

The last term of equation (43) is the incoherent term of mixing (Cotton, 1991*a*, 1999). It depends on the coherent scattering lengths of molecules and comes from the absence of correlation between the location of one molecule and its isotopic composition.

As an example, we have calculated the fraction x_{slvD} of D-benzene to be used in a blank sample for $c = 0.1$ g cm^{-3} of D-polystyrene (PSD) dissolved in H-benzene. Numerical data are given in Table 2. In this case, incoherent scattering predominates and the difference in compressibility terms between the solution and the solvent mixture can be neglected. The number of PSD molecules per unit volume of solution is $x_2/v_2 = \mathcal{N}_a c/m_{C_8D_8} = 5.38\times10^{20}$ cm^{-3}. The corresponding volume fraction is $x_2 = 8.74\times10^{-2}$. Thus, the number of solvent molecules per unit volume of solution is $x_1/v_1 = 1/v_1 - (x_2/v_1) = 6.17\times10^{21}$ cm^{-3}. The incoherent scattering of the solution is $\tilde{\sigma}^{inc}_s = (a^{inc}_{C_6H_6})^2 x_1/v_1 + (a^{inc}_{C_8D_8})^2 x_2/v_2 = 0.237$ cm^{-1}. The composition of the mixture having this incoherent cross section is obtained by solving equation (43). The positive solution of this equation is $x_{slvD} = 0.28$. Note that this volume fraction of D-benzene is high compared with the concentration of the D-polymer (0.1 g cm^{-3}) in solution. This clearly shows the importance of composition fluctuations (Cotton, 1991*b*, 1999) in incoherent scattering of the solvent mixture.

Equation (43) assumes that no isotopic exchange between H and D molecules occurs. This is not the case in water, in which H_2O, D_2O, HDO and DHO coexist in the mixture. In this peculiar case, a correct calculation leads to

$$
\begin{aligned}
\tilde{\sigma}^{inc}_{water}\,v_{water} = {}& x_{slvD}(a^{inc}_{D_2O})^2 + (1-x_{slvD})(a^{inc}_{H_2O})^2\\
&+ x_{slvD}(1-x_{slvD})\big[4(a_D-a_H)^2\\
&+ 2(a_D+a_H+a_O)^2\big],
\end{aligned}
\tag{44}
$$

where a_D, a_H and a_O are the coherent scattering lengths of H, D and O nuclei. The 'incoherent' scattering signal is increased

since the mixture contains more than two species. Equation (44) rectifies an oversight of Cotton (1991*a*) and corrects a mistake of Cotton (1999).

References

Brandrup, J. & Immergut, E. H. (1989). Editors. *Polymer Handbook*. New York: Wiley Interscience.

Calmettes, P. (1999). *J. Phys. IV*, **9**, 83.

Cotton, J. P. (1991*a*). *Neutron, X-ray and Light Scattering*, edited by P. Linder & T. Zemb, ch. 1, pp. 3–31. Amsterdam: North Holland.

Cotton, J. P. (1991*b*). *Neutron, X-ray and Light Scattering*, edited by P. Linder & T. Zemb, ch. 2, pp. 19–31. Amsterdam: North Holland.

Cotton, J. P. (1999). *J. Phys. IV*, **9**, 21–49.

Cotton, J.-P., Farnoux, B. & Jannink, G. (1972). *J. Chem. Phys.* **57**, 290–294.

Cotton, J.-P., Ober, R. & Roth, M. (1974). Lecture notes available at Laboratoire Léon Brillouin, CEA-Saclay, France.

Feigin, L. & Svergun, D. (1987). *Structure Analysis by Small-Angle X-ray and Neutron Scattering*. New York: Plenum Press.

Fourmaux-Demanges, V. (1998). PhD thesis, Université Paris XI, France.

Ghosh, R. & Rennie, A. (1999). *J. Appl. Cryst.* **32**, 1157–1163.

Glatter, O. (1977). *J. Appl. Cryst.* **10**, 415–c421.

Glinka, C. J., Barker, J. G., Hammouda, B., Krueger, S., Moyer, J. J. & Orts, W. J. (1998). *J. Appl. Cryst.* **31**, 430–445.

Guinier, A. (1964). *Théorie et Technique de la Radiocristallographie*. Paris: Dunod.

Higgins, J. C. & Benoît, H. C. (1994). *Polymers and Neutron Scattering*. Oxford: Clarendon Press.

Horkay, F., Hecht, A.-M., Mallam, S., Geissler, E. & Rennie, A. (1991). *Macromolecules*, **24**, 2896–2902.

Jacrot, B. (1976). *Rep. Prog. Phys.* **39**, 911–953.

Jacrot, B. & Zaccaï, G. (1981). *Biopolymers*, **20**, 2413–2426.

Kostorz, G. (1979). *Treatise on Materials Science and Technology*, Vol. 15, ch. *Neutron Scattering*, pp. 227–289. London: Academic Press.

Lairez, D. (1999). *J. Phys. IV France*, **9**, 67–81.

Lairez, D. (2006). http://www-llb.cea.fr/pace/pasidur.html.

Lide, D. R. (1995–1996). Editor. *Handbook of Chemistry and Physics*, 76th ed. Boca Raton: CRC Press.

Lindner, P. (2002). *Neutrons, X-rays and Light Scattering*, edited by P. Lindner & T. Zemb, pp. 23–48. Amsterdam: North Holland.

Lindner, P., Leclercq, F. & Damay, P. (2000). *Physica B*, **291**, 152.

May, R., Ibel, K. & Haas, J. (1982). *J. Appl. Cryst.* **15**, 15–19.

Monkenbusch, M. (1991). *J. Appl. Cryst.* **24**, 955–958.

Pedersen, J. S., Posselt, D. & Mortensen, K. (1990). *J. Appl. Cryst.* **23**, 321–333.

Ragnetti, M., Geiser, D., Höcker, H. & Oberthür (1985). *Makromol. Chem.* **186**, 1701.

Rawiso, M., Duplessix, R. & Picot, C. (1987). *Macromolecules*, **20**, 630.

Russell, T. P., Lin, J. S., Spooner, S. & Wignall, G. D. (1988). *J. Appl. Cryst.* **21**, 629–638.

Schelten, J. & Schmatz, W. (1980). *J. Appl. Cryst.* **13**, 385–390.

Schmatz, W., Springer, T., Schelten, J. & Ibel, K. (1974). *J. Appl. Cryst.* **7**, 96–116.

Sears, V. (1992). *Neutron News*, pp. 26–37.

Strunz, P., Saroun, J., Keiderling, U., Wiedenmann, A. & Przenioslo, R. (2000). *J. Appl. Cryst.* **33**, 829–833.

Stuhrmann, H. B. (1974). *J. Appl. Cryst.* **7**, 173–178.

Wignall, G. D. & Bates, F. S. (1987). *J. Appl. Cryst.* **20**, 28–40.